J Mater Sci (2010) 45:765–770
DOI 10.1007/s10853-009-3998-2

A visualization of shear strain in processing by high-pressure torsion

Y. Cao · Y. B. Wang · S. N. Alhajeri · X. Z. Liao · W. L. Zheng · S. P. Ringer · T. G. Langdon · Y. T. Zhu

Received: 3 September 2009 / Accepted: 27 October 2009 / Published online: 10 November 2009

Abstract Optical microscopy was used to examine the shear strain imposed in duplex stainless steel disks during processing by high-pressure torsion (HPT). The results show a double-swirl pattern emerges in the early stages of HPT and the two centres of the swirl move towards the centre of the disk with increasing revolutions. Local shear vortices also develop with increasing numbers of revolutions. At 20 revolutions, there is a uniform shear strain pattern throughout the disk and no local shear vortices.

Y. Cao · Y. B. Wang · X. Z. Liao (✉)
School of Aerospace, Mechanical and Mechatronic Engineering, The University of Sydney, Sydney, NSW 2006, Australia
e-mail: xliao@usyd.edu.au

S. N. Alhajeri · T. G. Langdon
Materials Research Group, School of Engineering Sciences, University of Southampton, Southampton SO17-1BJ, UK

W. L. Zheng
Shanghai Research Institute of Materials, 99 Handan Road, Shanghai 200437, China

S. P. Ringer
Australian Key Centre for Microscopy & Microanalysis, The University of Sydney, Sydney, NSW 2006, Australia

T. G. Langdon
Departments of Aerospace and Mechanical Engineering and Materials Science, University of Southern California, Los Angeles, CA 90089-1453, USA

Y. T. Zhu
Department of Materials Science and Engineering, North Carolina State University, Raleigh, NC 27695, USA

Introduction

Processing through the application of severe plastic deformation (SPD) is now widely used for the production of bulk ultrafine-grained (<1 μm) and nanocrystalline (<100 nm) materials [1–3] having superior mechanical properties including a combination of high strength and good ductility at ambient temperature [4, 5] and a superplastic forming capability at elevated temperatures [6]. The processing of metals by torsionally straining under a compressive force was first proposed more than 60 years ago in the classic work of Bridgman [7] but now, amongst all SPD techniques, high-pressure torsion (HPT) is attracting considerable attention because it is exceptionally effective in producing grain refinement in bulk solids [1, 3, 8–10].

The samples processed by HPT are normally in the shape of disks. For the ideal rigid-body situation, the shear strain, γ, imposed on a disk by HPT, which plays a key role in grain refinement, may be calculated using the equation $\gamma = 2\pi Nr/h$, where N denotes the number of revolutions, r is the distance from the centre of the disk and h is the disk thickness. The following conclusions may be drawn from this relationship: (1) the shear strain direction at any position in the disk is perpendicular to the radial direction at that position, (2) the shear strain, and therefore the measured hardness, should be the same at all points having the same radial value and (3) the shear strain at the centre of the disk is zero. However, there are numerous reported deviations from this simple interpretation [11–15] and there are proposed mechanisms to explain these deviations. For example, observations of an undulating microhardness evolution led to the proposal that deformation develops in a repetitive manner throughout the outer ring of the disk and thereafter the shearing spreads inwards towards the centre

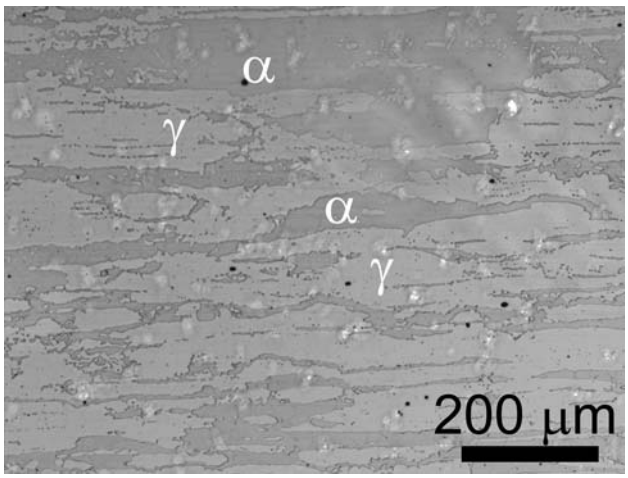

Fig. 1 A typical optical image of the as-received duplex stainless steel. The γ and α phases are indicated in the image

[11]. A detailed analytical model was developed to explain the formation of a uniform microstructure in HPT disks after processing through large numbers of revolutions [16]. Despite these advances, there has been no attempt to date to make use of optical microscopy to critically assess the deformation characteristics imposed by HPT. The present investigation uses optical microscopy and demonstrates there are significant local deviations in the imposed shear strains from those anticipated using an ideal rigid-body analysis.

Since most of the earlier investigations of HPT were conducted using single-phase materials [17–19] or multi-phase alloys with only a small amount of second phase [20, 21], it was difficult to clearly visualize the shear strain imposed during HPT. By choosing a duplex stainless steel in the present investigation, in which roughly the same volume fraction of austenite (γ phase) and ferrite (α phase) coexist, it was possible to visualize the shear strain directly from the optical images. In practice, these γ and α phases appear in the optical images as white and black areas or domains, respectively [22]. An example of a typical optical image of the as-received duplex stainless steel used in this investigation is shown in Fig. 1, in which grains of both the γ phase and the α phase are elongated with very large aspect ratios along the rolling direction of the as-received material and the widths of the two phases vary approximately from 20 to 100 μm.

Experimental

Disks with a thickness of 0.79 mm and a diameter of 9.8 mm were processed using quasi-constrained HPT [3] under applied pressures of 6.0 GPa through 2, 3 and 5 revolutions or 4.0 GPa through 20 revolutions, respectively. The thickness was reduced to about 0.77 mm after HPT. The rotation speed was set at one revolution per minute. X-ray diffraction of the HPT disks detected no phase transformations. Samples were prepared for optical microscopy investigation by polishing the bottom surfaces of the disks using 6 and 1 μm diamond lapping films and then chemically etching using a solution of 45% water, 30% nitric acid, 10% hydrofluoric acid and 15% hydrochloric acid. This polishing and etching process removed a surface layer $\sim$70 μm in thickness. The optical imaging was performed using an Olympus BX60 motorized optical microscope. A Philips CM12 transmission electron microscope (TEM) operating at 120 kV was employed to examine the HPT structures. A TEM specimen was prepared by cutting a 3 mm diameter disk from near the edge of an HPT disk, grinding to $\sim$100 μm thickness and then electro-polishing at room temperature using a Struers Tenupol 5 jet thinner and a solution of 23% perchloric acid and 77% acetic acid under a 20 V working voltage.

Results

Figure 2a shows an optical image of the 2-revolution HPT disk. An irregular macroscopic shear strain is clearly seen along the coarse lighter track which is marked with four white arrows at the two ends and at two sharp turning points, respectively. At this stage of the deformation, only a small amount of shear strain has been imposed at the central part of the disk marked B in Fig. 2a, where this area is shown in a magnified image in Fig. 2b. It is interesting to note that the shear strain direction in the area marked C in Fig. 2a lies roughly parallel to the radial direction of the region, as is also evident in the magnified image of the same area shown in Fig. 2c.

The strong deviation of shear strain from the ideal rigid-body situation in the 2-revolution HPT disk is attributed to deviations of the directions of local frictional forces from the ideal situation where these forces should lie perpendicular to the radial direction at every point. Possible explanations for these deviations include (1) a slippage between the disk and the HPT anvils during the HPT process where this is known to become increasingly significant for hard materials such as the duplex stainless steel [23], (2) variations in the local thickness of the disk from point to point across the diameter and (3) local variations in surface roughness between the disk and the HPT anvils.

With an increase in the number of revolutions, the influence of variations in thickness and surface roughness is reduced and the effect of any slippage becomes negligible [23]. Therefore, it is reasonable to anticipate that the shear strain imposed by HPT will gradually approach the ideal situation with increasing HPT revolutions. This is the

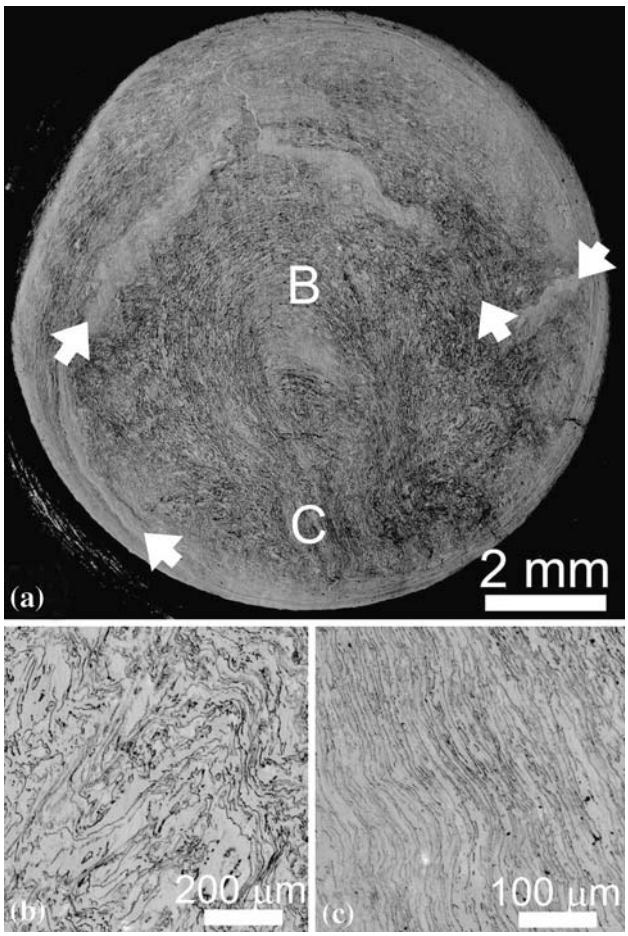

Fig. 2 **a** An optical image of the 2-revolution HPT disk: four *white arrows* indicate the two ends and two sharp turning points of an irregular macroscopic shear strain track. **b** A magnified image of the central area marked B in **a**. **c** A magnified image of the area marked C in **a**

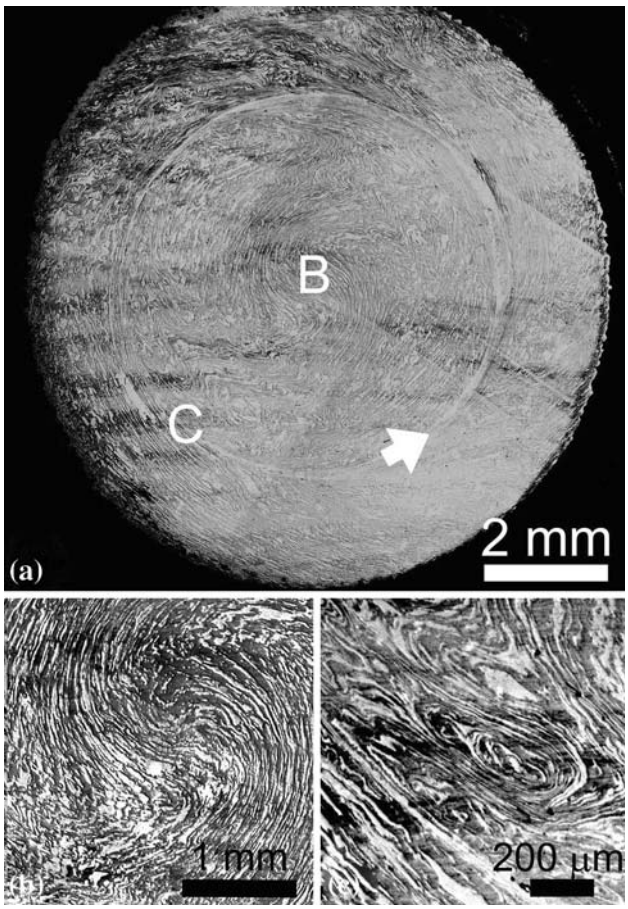

Fig. 3 **a** An optical image of the 5-revolution HPT disk: a *white arrow* indicates a circular macroscopic shear strain track. **b** A magnified image of the central area marked B in **a**. **c** A magnified image of the area marked C in **a**

case for the 5-revolution disk as shown by the optical image in Fig. 3a. In this sample there is a clear circular macroscopic shear strain with the centre of the circle corresponding with the centre of the disk and the radius of the circle having a value of about 2/3 of the disk radius: this circle is marked with a white arrow. The circular macroscopic shear strain demonstrates that the strain imposed by HPT is much closer to the ideal state in the 5-revolution disk than in the 2-revolution disk. However, careful analysis revealed the presence of a unique double-swirl pattern of shear strain in the central region of the disk at B as revealed clearly by the higher magnification image in Fig. 3b. Measurements showed the distance between the two centres of the double-swirl was ~ 1 mm and the centre of the double-swirl, which was located by determining the mid-point of a straight line connecting the two centres of the individual swirls, coincided with the centre of the HPT disk within experimental accuracy. It is important to note that the alternating black and white domains at the disk centre in Fig. 3b are severely elongated and thereby confirm the imposition of large shear strains within the vicinity of the centre of the 5-revolution disk.

Another significant feature of shear strain in the 5-revolution disk is the presence of small local shear vortices that are visible at many places throughout the disk. An example is present at the point labelled C in Fig. 3a and shown in an enlarged image in Fig. 3c. A careful examination of many vortices suggests these vortex areas incorporate larger shear strain than their surrounding areas as indicated by the thinner black and white domain areas. The formation of local shear vortices may be related to hardness variations due to local differences in the grain size. During the plastic deformation of the duplex steel, shear instabilities could also develop and contribute to the observed inhomogeneous deformation pattern. Since these local vortices are not present in the initial stages of HPT deformation as in Fig. 2, variations in the macroscopic disk thickness and surface roughness cannot account for their formation. A local vortex structure was also reported in

pearlite processed by HPT where ferrite and cementite phases coexist [24], thereby suggesting that this may be a common feature at least in two-phase materials, where there are comparable volume fractions of each phase, processed by HPT.

A comparison of the shear strain patterns of the 2-, 3- and 5-revolution HPT disks indicated that the 3-revolution HPT disk was intermediate in structure between the 2- and 5-revolution disks. Thus, the shear strain in the 3-revolution HPT disk was less irregular than in the 2-revolution HPT disk although there was some evidence for a shear strain direction parallel to the local radial direction. Furthermore, the double-swirl shearing pattern started to form and two local shear vortices were visible with sizes larger than in the 5-revolution disk. However, the double-swirl pattern was not as clear as in the 5-revolution disk.

Experiments showed further increases in the number of revolutions produced a more uniform structure throughout the disks and eliminated the local vortices. An example is given in Fig. 3 for the HPT disk taken through 20 revolutions. For this sample, the double-swirl pattern is again evident, the centre of the double-swirl coincides with the centre of the disk but the distance between the two centres of the double-swirl is reduced to $\sim$150 μm. Most of the shear strain directions throughout the disk now lie parallel to the circumference of the disk and this is consistent with the ideal rigid-body interpretation of strain. It follows, therefore, that at relatively large numbers of revolutions the situation approximates to the ideal such that the local deviations in shear strain no longer exist.

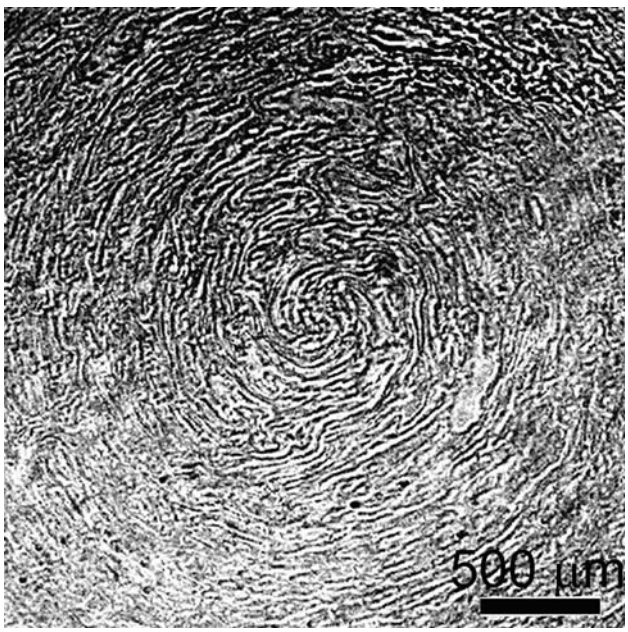

Fig. 4 An optical image of the central area of the 20-revolution HPT disk

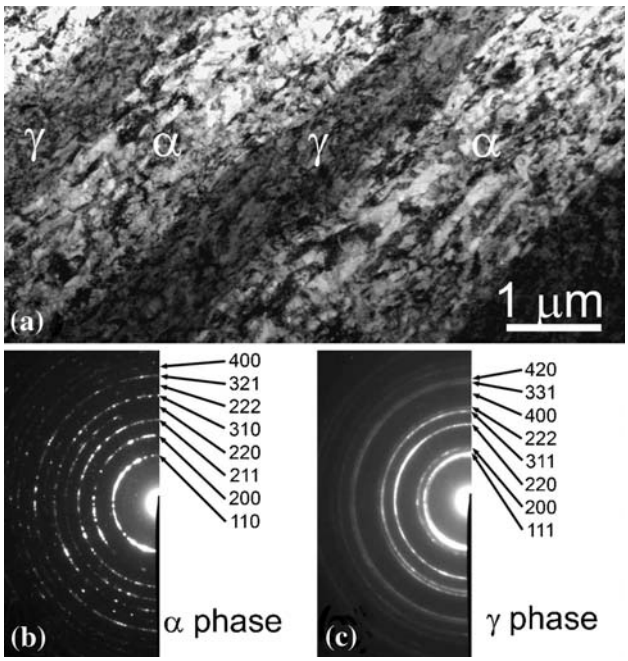

Fig. 5 **a** A TEM image of alternating black and white domains in a sample processed through 20 HPT revolutions. **b** An indexed electron diffraction pattern of a white domain, and **c** an indexed electron diffraction pattern of a black domain indicating they are mainly the body-centred cubic α phase and the face-centred cubic γ phase, respectively: note that the white and black domains in TEM are opposite to those in an optical image

It is important to note that, except for the case of the as-received sample, each white or black domain visible in Figs. 2, 3 and 4 corresponds to a region of multiple grains. Thus, nanocrystalline grains were clearly visible in the white/black domain areas in the disk taken through 20 revolutions. An example is shown in the TEM image in Fig. 5a where the electron diffraction patterns obtained from white and black areas are separately indexed and shown in Fig. 5b, c, respectively. The indices of the electron diffraction patterns confirm that the white and black domains are composed mainly of the body-centred cubic α phase and the face-centred cubic γ phase, respectively. This result is consistent with the X-ray diffraction analysis showing an absence of any strain-induced phase transformations.

Discussion

The swirling shear strain patterns observed in this study are not unique to duplex stainless steel. Careful inspection reveals that swirling shear strains were observed in other materials processed by HPT including pure Al [25, 26] but that the shear strains in single-phase materials are less apparent than in duplex stainless steel. It is reasonable to conclude that the poor contrast of the swirling shear strain

in pure metals and other materials has led to a general ignorance of this phenomenon.

The occurrence of swirling is a well-known and common phenomenon in nature. It is seen in galaxy patterns [27, 28], in fluid dynamic patterns such as the vortices formed behind a rotating propeller [29] and in equivorticity lines under certain circumstances [30]. Recent computer simulations of plasma turbulence have revealed double-swirl patterns and their evolution that are surprisingly similar to those reported here in the central region of HPT duplex stainless steel disks [http://www.princeton.edu/artofscience/2009/one.php%3Fid=1058.html]. Nevertheless, the swirling of shear strain in HPT materials was an unexpected phenomenon and further investigations are now needed to provide a mechanism that accurately predicts the formation of this swirling in materials imposed by HPT.

Vortex microstructures similar to those seen in this investigation were also observed in the weld zone of friction stir welded copper and aluminium [31–33] and in the shear band patterns in metals deformed at high strain rates [34]. The creation of local vortices in the friction stir weld zone was explained as a result of the difference in local shear stain rates and strain directions introduced by the rotating pin. Vortex shear band patterns formed within metals deformed at high rates appear to be related to the instability of laminar flow of the material within the shear band which resembles that of a viscous fluid confined between two rigid plates moving parallel to each other [34].

Local vortices can occur in continuous fluids with velocity variations or in two fluids with sufficient velocity difference across the interface of the fluids. This phenomenon is called Kelvin–Helmholtz instability [35, 36]. A similar shear velocity difference may also occur locally in the HPT process of the duplex stainless steel because of the local structural difference, indicating that the development of local vortices could be correlated to the Kelvin–Helmholtz instability in fluids.

The simple shear strain equation of $\gamma = 2\pi Nr/h$ was developed mathematically for a rigid-body situation but it is now apparent that local microstructural effects lead to variations from point-to-point within any bulk polycrystalline solid and this introduces deviations from the theoretical relationship which are not easily included in a mathematical model.

Conclusions

1. The shear strain in two-phase duplex stainless steel disks processed by HPT was successfully examined using optical microscopy. The results show that the shear strain deviates from the ideal rigid-body model in the initial stages of HPT but that this deviation gradually disappears with increasing numbers of HPT revolutions.
2. Two phenomena occur with increasing revolutions. First, a double-swirl shear strain pattern emerges where the two centres of the double-swirl attract each other and move towards the centre of the HPT disk. Second, there are local shear strain vortices that become apparent at low numbers of revolutions but ultimately are lost after large numbers of turns. The observed shear strain evolution provides new insight into the straining processing and should be incorporated into any detailed model of grain refinement in HPT processing.

Acknowledgements The authors are indebted to Professor J. T. Wang for his extensive discussion of swirling phenomena in nature and they are grateful for scientific and technical input and support from the Australian Microscopy & Microanalysis Research Facility node at the University of Sydney. This project was supported by the Australian Research Council [Grant No. DP0772880 (Y.C., Y.B.W., and X.Z.L.)], the US Army Research Office (Grant No.W911NF-08-1-0201, T.G.L.) and the U.S. DOE IPP program (Y.T.Z.).

References

1. Valiev RZ, Islamgaliev RK, Alexandrov IV (2000) Prog Mater Sci 45:103
2. Valiev RZ, Langdon TG (2006) Prog Mater Sci 51:881
3. Zhilyaev AP, Langdon TG (2008) Prog Mater Sci 53:893
4. Valiev RZ, Alexandrov IV, Zhu YT, Lowe TC (2002) J Mater Res 17:5
5. Wang YM, Chen MW, Zhou FH, Ma E (2002) Nature 419:912
6. Horita Z, Furukawa M, Nemoto M, Barnes AJ, Langdon TG (2000) Acta Mater 48:3633
7. Bridgman PW (1943) J Appl Phys 14:273
8. Liao XZ, Zhao YH, Zhu YT, Valiev RZ, Gunderov DV (2004) J Appl Phys 96:636
9. Liao XZ, Zhao YH, Srinivasan SG, Zhu YT, Valiev RZ, Gunderov DV (2004) Appl Phys Lett 84:592
10. Sabirov I, Pippan R (2005) Scripta Mater 52:1293
11. Zhilyaev AP, Nurislamova GV, Kim BK, Baró MD, Szpunar JA, Langdon TG (2003) Acta Mater 51:753
12. Zhilyaev AP, Oh-ishi K, Langdon TG, McNelley TR (2005) Mater Sci Eng A 410:277
13. Xu C, Horita Z, Langdon TG (2007) Acta Mater 55:203
14. Xu C, Horita Z, Langdon TG (2008) Acta Mater 56:5168
15. Todaka Y, Umemoto M, Yin J, Liu Z, Tsuchiya K (2007) Mater Sci Eng A 462:264
16. Estrin Y, Molotnikov A, Davies CHJ, Lapovok RJ (2008) J Mech Phys Solids 56:1186
17. Jiang H, Zhu YT, Butt DP, Alexandrov IV, Lowe TC (2000) Mater Sci Eng A 290:128
18. Zhilyaev AP, Lee S, Nurislamova GV, Valiev RZ, Langdon TG (2001) Scripta Mater 44:2753
19. Yang Z, Welzel U (2005) Mater Lett 59:3406
20. Kai M, Horita Z, Langdon TG (2008) Mater Sci Eng A 488:117
21. Rajulapati KV, Scattergood RO, Murty KL, Horita Z, Langdon TG, Koch CC (2008) Metall Mater Trans A 39A:2528

22. Johansson J, Odén M (2000) Metall Mater Trans A 31A:1557
23. Edalati K, Horita Z, Langdon TG (2009) Scripta Mater 60:9
24. Ivanisenko Y, Lojkowski W, Valiev RZ, Fecht H-J (2003) Acta Mater 51:5555
25. Sakai G, Horita Z, Langdon TG (2005) Mater Sci Eng A 393:344
26. Kawasaki M, Langdon TG (2008) Mater Sci Eng A 498:341
27. Bertin G (2000) Dynamics of galaxies. Cambridge University Press, Cambridge, UK
28. Binney J, Tremaine S (2008) In: Spergel DN (ed) Galacitic dynamics, 2nd edn. Princeton University Press, Princeton, NJ, USA
29. Van Dyke M (1982) An album of fluid motion. The Parabolic Press, Stanford, CA, USA
30. Zeytounian RKh (2004) Theory and applications of viscous fluid flows. Springer-Verlag, Berlin, Germany
31. Murr LE, Li Y, Flores RD, Trillo EA, McClure JC (1998) Mat Res Innov 2:150
32. Zhang HW, Zhang Z, Chen JT (2007) J Mater Process Technol 183:62
33. Zhang Z, Chen JT (2008) J Mater Sci 43:222. doi:10.1007/s10853-007-2129-1
34. Guduru PR, Ravichandran G, Rosakis AJ (2001) Phys Rev E 64:036128
35. Kelvin (1871) Lord (William Thomson) Phil Mag 42: 362
36. von Helmholtz HLF (1868) Monthly Reports of the Royal Prussian Academy of Philosophy (Berlin) 23:215